# Mechanisms of Mixing and Creation of Structure in Laminar Stirred Tanks

**M. M. Alvarez, J. M. Zalc, T. Shinbrot, P. E. Arratia, and F. J. Muzzio**
Dept. of Chemical and Biochemical Engineering, Rutgers University, Piscataway, NJ 08855

*Although stirred tanks have been the most commonly used fluid mixing devices since the beginnings of the industrial era, little is known about how and why they mix, and, therefore, about how to improve their performance, particularly when operated in the laminar regime. In laminar conditions, chaos is the only route to achieve efficient mixing. From the body of research in 2-D chaotic flows, very minute perturbations in the velocity field can lead to widespread chaos and substantial enhancement of mixing performance, but these observations have not been systematically applied to industrially relevant 3-D flows. Using planar laser induced fluorescence and direct numerical simulations, the mechanisms of creation and evolution of mixing structures were studied in Newtonian and non-Newtonian flows. The observed dynamical behaviors are related to geometric features of the system. In Newtonian flow systems, the passing of the impeller blades triggers the onset of chaos by introducing small perturbations to the underlying regular 2-D flow that is observed when impellers are substituted with discs. In non-Newtonian viscoelastic systems, nonlinearity in the stress field introduced by the fluid rheology drives the system to spontaneous chaos even when concentric discs are used to stir the fluid.*

## Introduction

### *Motivation*

Fluid mixing operations are central to many industrial processes, ranging from those in which two miscible liquids are blended together to those involving complex chemical reactions, multiphase flows, non-Newtonian behavior, and so on. Driven by empriricism rather than by basic knowledge, industrial mixing is still considered by many to be more an ''art'' than a science. Our lack of fundamental knowledge of the physics of mixing in industrial systems has a price: a decade ago, it was estimated that perhaps 10 billion dollars/year were lost by North American industry due to mixing problems (Harnby et al., 1992). Consensus among practitioners is that little effective change has happened since then.

We center our discussion here on the most widely used piece of mixing equipment: the stirred tank. Everyday products such as detergents, creams, drugs and plastics are processed in stirred vessels during one or several steps of their manufacture. As an example, key pharmaceutical products like insulin, hepatitis B vaccine, interferon, penicillin, and so on are processed in stirred tanks. The scale and the geometry of a stirred tank can vary from 0.5 L vessels agitated by a single impeller (such as used to analyze dissolution of pharmaceutical tablets) to $10^8$ L tanks stirred by multiple impeller used to treat municipal effluents or to store (and, hopefully, process) nuclear waste.

In this article, we use experimental and computational methods to investigate the fundamental mechanisms of mixing in stirred tanks. We focus on the low Reynolds number regime, both because this situation arises in many practical applications (such as culture of shear-sensitive cells or micellium broths, and manufacture of creams and detergent) causing what practitioners consider to be ''the worst'' mixing problems, and because the steady flows characteristic of laminar processes greatly facilitate both modeling and experimentation, thus providing an excellent starting point for solid progress.

Correspondence concerning this article should be addressed to F. J. Muzzio.

### *Chaos and regularity in a stirred tank*

It has been well established, both experimentally and computationally, that efficient convective mixing in stirred tanks operated in laminar flow conditions is only possible in the presence of chaos (Lamberto et al., 1996; Lamberto, 1997; Harvey et al., 2000). Several authors have examined the interplay between chaos and convective mixing in model systems including two-dimensional (2-D) integrable and nonintegrable flows (Aref, 1984; MacKay, 1984; Ottino, 1989; Wiggins, 1992), and 3-D volume preserving systems (MacKay, 1994; Fountain et al., 1998). This body of research has led to fundamental improvements in our understanding of the generic mechanisms by which chaos leads to mixing in laminar systems.

Chaos is a consequence of reorientation of particle trajectories in time; however, although it is natural to suspect that this reorientation is related to the source of motion (the impeller), the mechanism by which chaos is generated in conventional stirred tanks has not been described previously. In fact, the development of structure due to the mixing process in stirred tank systems has not been studied in detail and connections between geometrical features of the tank and dynamical mixing behavior have not been elucidated.

In the laminar regime, the flow produced by conventional impellers is mainly radial. Even so-called ''axial'' impellers originate a radial flow when used in laminar conditions (see, for example, Harvey III et al., 1995; Lamberto et al., 1996). This causes mixing pathologies that are well known to practitioners: establishment of transport separatrices at impeller mid-planes, and generation of toroidal regions of circulatory motion above and below the impeller planes (see, for example, Metzner and Taylor, 1960). However, studies have only recently addressed these problems in detail. Lamberto et al. (1996, 2000) observed experimentally and computationally that these circulatory regions are in fact regions of regular motion isolated from the remainder of the flow domain, wherein motion is chaotic. No exchange of material other than by diffusion was possible between the chaotic and regular regions.

The analogies between stirred tanks and 2-D model flow systems extend further than the co-existence of chaos and regularity. The deformation of interfaces under chaotic conditions in 2-D flows generates a very complicated lamellar pattern (partially mixed structure) that displays a very wide distribution of length scales. At every position of the chaotic flow domain, there exists a defined manifold orientation. The lamellar structure is rapidly attracted exponentially to the global unstable manifold of the flow system and evolves according to a basic template that is invariant in time (property known as asymptotic directionality: see Muzzio et al. (2000)). This process of development of striation patterns (described in detail for 2-D flows in Alvarez et al. (1998) and Alvarez (2000)) is also observed in stirred tanks.

This article explores the process of the creation of structure in several stirred tank configurations using experimental and computational techniques. The main objective is to elucidate the mechanisms that trigger chaos in stirred tanks. Dynamical Systems literature extensively documents that time-periodic perturbations can introduce chaos in an otherwise regular 2-D system (see, for example, Aref, 1984; Ottino, 1989; Beigie et al., 1994; Hobbs et al., 1997; Alvarez et al., 1998). Stirred tanks are a particular 3-D extension of this phenomenon and identify the precise source of these perturbations in the 3-D concentric tank. It is shown using the following approach.

First, we study a stirred tank system with a single Rushton impeller mounted in a central shaft. Using UV visualization techniques, we illustrate the 3-D mechanism by which fluorescent dye is dispersed within the chaotic region of the tank. Second, we compare a system with three Rushton impellers with a system with three discs at the same locations. While the first system displays the co-existence of regular and chaotic motion, the second one cannot display chaos since, due to azimuthal symmetry, it is effectively a 2-D integrable system. Through detailed comparison between the impeller and disk systems, we find that chaos is originated by the folding of material lines caused by the periodic passing of the blades. These blades perturb only weakly the underlying regular flow of the three disc system. Experiments with modified Rushton turbines demonstrate that the frequency and amplitude of the perturbation, and the resulting mixing behavior observed in the three-Rushton case, are strongly dependent on the geometry of the impeller.

Additionally, we briefly address non-Newtonian scenarios, where spontaneous elastic oscillations introduced by fluid rheology trigger chaos even in 2-D systems gently agitated by concentric discs.

## Experimental Techniques

### *Apparatus*

For all experiments reported here, we used flat-bottom transparent acrylic cylindrical vessels (17 in. high and 9.5 in. diameter) with small conical depressions at the bottom to anchor the impeller shaft (see Figure 1). The tanks were surrounded by a rectangular fluid-filled chamber to minimize optical aberration due to curvature of the tank walls.

Two different stirrer geometries are used: acrylic discs (7.623 cm [3 in.] diameter and 0.635 cm thick) and Rushton impellers (7.623 cm [3 in.] diameter from blade tip to blade tip). The Rushton impellers used here consist of a 5.082 cm [2 in.] diameter disc with six 1 $cm^2$ square blades mounted equally spaced and perpendicularly, such that half of their surface is above, and half is below, the mid-plane defined by the disc. Two modified Rushton geometries are also used, one in which the second, fourth, and fifth blades are removed (Figure 1e), and another in which the first blade is displaced above the mid-plane and the second below the mid-plane. Two different shaft-impeller setups are used: a single stirrer (disc or Rushton) located 10.164 cm (4 in.) above the bottom in tanks with an aspect ratio of 1.25 (see Figure 1a); and three stirrers mounted in the same shaft at 8.893, 17.787 and 26.680 cm (3.0, 5.0, and 10.5 in. respectively) above the bottom in a tank with an aspect ratio of 1.5 (Figure 1b).

### *Working fluids*

Glycerin is used as a Newtonian working fluid (99.7% pure, USP Kosher, B.R.O.W.N. Chemical Company, Inc., Paterson, NJ). As a non-Newtonian model fluid, we used 1% Car-

boxy-methyl-cellulose solutions in water (a weakly viscoelastic, strongly shear thinning fluid with low yield stress (Nienow and Elson, 1988)). The rheological characterization of 1% CMC solutions was performed with an automatic plate and cone rheometer (SR-2000 from Rheometric Scientific).

### *UV light visualization*

Fluorescent tracer experiments using Rhodamine G and Fluorescein are carried out to reveal 3-D mixing patterns using UV light in an otherwise dark room. A UV lamp emitting at 365 nm (Model XX-15A, 120 V, 60 Hz) is located above the experimental station to provide illumination, and a 35 mm camera (Pentax K-1000) is used to take photographs.

### *Planar laser-induced fluorescent experiments*

A laser illumination technique is used to reveal mixing structures at specific 2-D planes within the stirred tanks. The experimental system is illuminated with a YAG laser sheet (1 mm thickness; wavelength = 535 nm) in an otherwise dark room, and the mixing structure of the illuminated 2-D plane is revealed by injecting a fluorescent tracer. Images of the illuminated plane are captured on 35 mm slide film using the photographic camera mentioned earlier (Figure 2).

Rhodamine G dissolved in glycerin serves as a passive tracer (once its bouyancy has been properly matched with that of the fluid in the tank) to reveal the manifold structures.

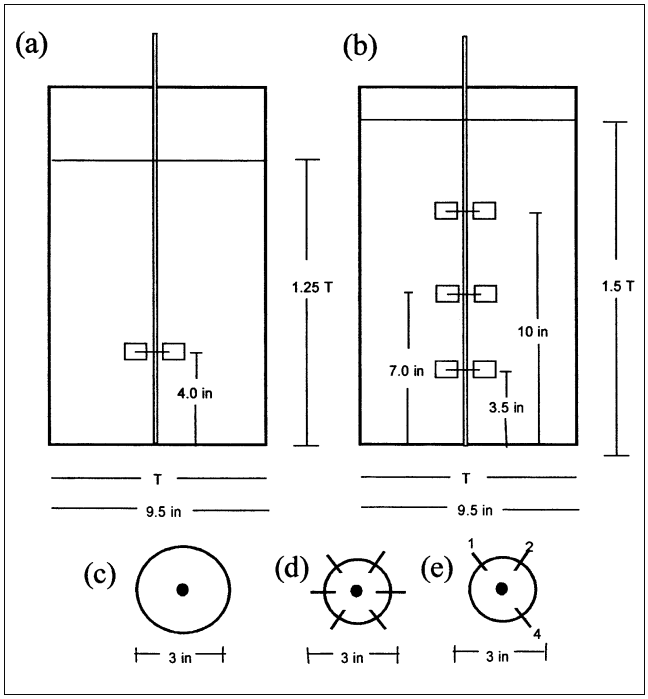


**Figure 1. Experimental setup.**

Systems with (a) one, and (b) three impeller systems are investigated. Three impeller designs are used: (c) 3 in. diameter discs, (d) six blade Rushton turbines, and (e) modified Rushton turbines.

## Computational Techniques

Several software tools are used to numerically simulate mixing performance in stirred tanks. This includes tools for parametric geometry definition, unstructured tetrahedral meshing, flow field solution, and Eulerian and Lagrangian post-processing routines. In this section, only a brief description of the computational techniques used in this work is presented. Details are provided in Zalc (2000) and Zalc et al. (2001).

### *Calculation of velocity fields.*

Once the discretization of the flow domain has been performed (using ICEM-CFD, Berkley, CA), the CFD velocity field solver (acuSolve from ACUSIM Software, Saratoga, CA) is used to obtain values for the velocity components and pressure at each of the node points. The solver uses a full finite-element formulation to solve the fully-coupled mass and momentum conservation equations. The flow fields are solved in a rotating frame of reference in which the flow is time-independent. In each simulation, the solution is considered converged when the normalized residuals for the three velocity components and the pressure all fall below $10^{-4}$. The computations were run in parallel on eight HAL class 375 machines (Fujitsu, Campbell, CA). Calculation of the velocity and pressure fields for each Reynolds number ($Re$) takes between 75 and 200 iterations to converge and each run takes less than eight hours of CPU time on each of the eight processors.

**Figure 2. Experimental setup for acquisition of planar-laser induced fluorescence (p-LIF) images.**

A laser gun (1) projects a sheet of light (2) through the experimental system (3) in a dark room. A 35 mm. photographic camera (4), located perpendicular to the illuminated plane, is used to acquire images.

### *Poincaré Sections*

2-D return maps are computed in which the impellers remain still while the tank is spun. A lattice of 16 (radial) by 48 (vertical) particles is initially aligned with one of the impeller blades and covers half of the vertical cross-section of the stirred tank. The intersection surface chosen is a vertical plane extending from the shaft to the tank wall and aligned with one of the impeller blades. Particle trajectories are computed for 600 tank rotations by integration of the velocity field by a fifth-order Runge-Kutta algorithm.

Particle positions are recorded every time a particle crosses the intersection surface. All of the intersections are plotted on one graph to expose chaotic and regular regions (as will be shown in Figure 6).

### *Stretching contours*

A lattice of 60,000 equally spaced tracer particles covering the right half of the vertical cross-section of the tank is used as an initial condition. The evolution and rate of elongation of infinitesimal vectors ($l_o$) attached to each of these particles is calculated according to Eqs. 1 and 2

$$dl/dt = (\nabla v)^T \cdot l \tag{1}$$

$$\lambda = |l|/|l_o| \tag{2}$$

Fluid element trajectories and accumulated stretching values ($\lambda$) are computed for 20 impeller revolutions, and the initial particle positions are plotted with colors depending on the accumulated stretching (see Eq. 2).

## Results and Discussion

### *Dye dispersion in stirred tanks*

The creation of structure and the emergence of mixing patterns in stirred tanks can be investigated by tracer experiments. In chaotic systems, the unstable manifolds act as a template for transport of material (see, for example, Beigie et al., 1994). The processes of stretching and folding of fluid elements are constrained to the geometrical framework fixed by the unstable manifold structure, which itself is determined by the geometry of the system and the velocity field. Since the unstable manifold is uniquely defined for each particular chaotic flow, and since the mixture structure coincides with the manifold topology (Muzzio et al., 2000; see also Alvarez, 2000), the global geometrical features are revealed by the dispersion process independently of the injection point of tracer as far as this point belongs to the chaotic domain. Moreover, since the manifold has an invariant topology, the mixture structure evolves along a self-similar template, which greatly facilitates the study of the mixing process. However, depending on the branch or branches of the manifold at which an injection takes place, some features are revealed earlier than others.

We start our discussion analyzing a very simple experimental scenario. We follow the dispersion of fluorescent dye (fluorescein) in a glycerin/water solution (viscosity = 900cP) in an acrylic stirred tank agitated by a single Rushton impeller mounted on a central shaft (see Figure 3). The tank is operated in the laminar regime ($Re = 20$). An injection of neutrally buoyant dye is performed close to the shaft and 10 cm above the impeller. Figure 3a shows the earlier evolution of a fluorescent dye injection under UV light exposition. The stream of dye is convected toward the impeller, after which it is expelled by the blades toward the tank walls in a pattern of nested spirals (see Figures 3b and 3c). Near the walls, the dye ascends and forms envelopes that surround and enclose the regular regions (see Figure 3d). For the injection location and at the narrow time window illustrated in the figure (3 min), the dye disperses only in a region above the impeller plane. As dispersion progresses, the dye sheet continues its alignment to the invariant unstable manifold of the flow, increasingly filling in structural details. In Figure 3e a ribbon-like structure is observed 10 min after an injection slightly above the impeller plane and 3 cm from the tank wall. The early evolution of a second injection (red), this time performed at the impeller plane and 0.5 cm from the wall, is also shown (Figure 3f). While the green dye remains confined to the upper compartment of the tank, the red one spreads as a thin sheet close to the wall invading both tank compartments, revealing that, near the wall, the unstable manifold communi-

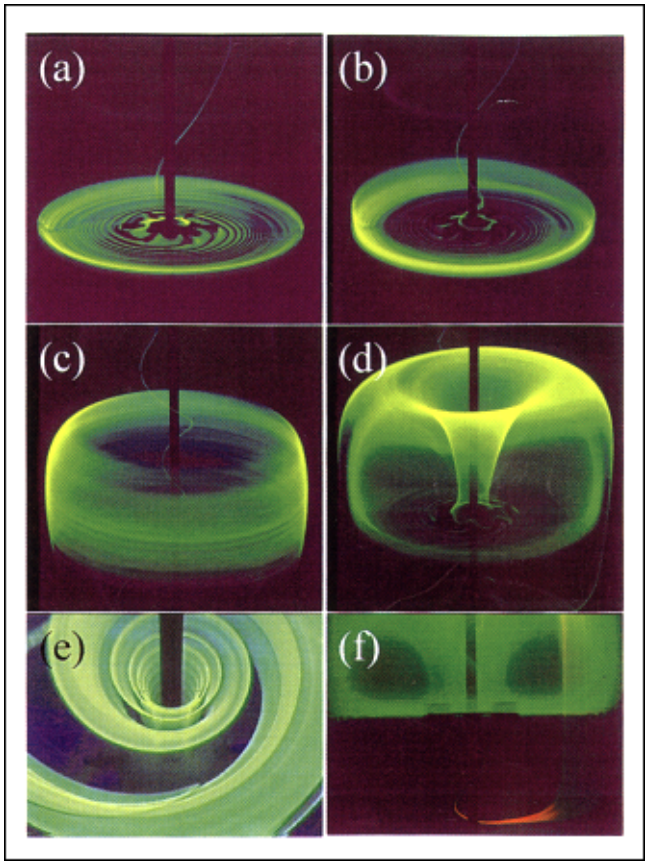


**Figure 3. Dispersion of fluorescent tracer in a stirred tank as revealed by a UV light visualization experiment.**

From (a) to (d), a sequence of snapshots is presented, showing the evolution of the 3-D structure originated by the stirring action of a single Rushton impeller in a tank at (a) 3, (b) 5, (c) 10, and (d) 30 s after injection of fluorescent tracer. (e) Helical ribbon observed 3 min after injection (top view). (f) Different manifold branches.

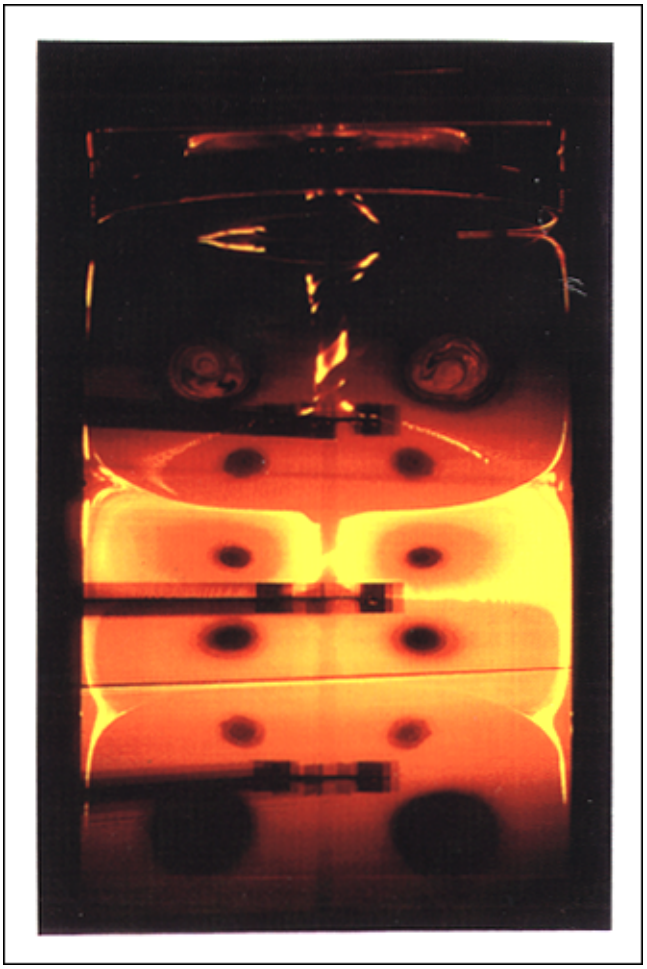

**Figure 4. P-LIF experiment revealing the flow structure in a three-Rushton system.**

cates the regions above and below the impeller plane. At later times (not shown), the red dye approaches the impeller in a pattern of spiral ribbons originated on the top and the bottom of the tank.

These 3-D visualizations render qualitative information about structure and transport in this simple stirred tank system. In particular, they uncover the role of the impeller blades as a ''source of 3-D stretching,'' the role of the velocity field near the shaft, causing the transport of material from the top and bottom of the tank to the impeller plane, and the nature of the transport processes between tank compartments by unstable manifold branches aligned with the tank walls. However, these visualizations are difficult to quantify, and have other intrinsic limitations. For example, the external manifold layers cover the internal ones, complicating further depth of analysis. In the next section we use planar laser induced fluorescence (p-LIF) to explore in detail the transport mechanisms in more complex stirred tank configurations.

### *Structure in a 3-Rushton impeller system*

As a second experimental system, we study a tank configuration widely used in fermentation applications: three Rushton impellers mounted on a central shaft. Since this system is geometrically more complicated than a single impeller system, intuitively, we expect a higher level of flow complexity and a wider repertoire of mixing behaviors. For example, at low speeds, we expect to find recirculation loops above and below each impeller (Harvey III et al., 1997), and perturbed separatrices at each impeller mid-plane and at midpoints between impellers.

The global features of the flow in a three-Rushton impeller system are unveiled by a triple injection p-LIF experiment (see Figure 4). Rhodamine is injected first slightly above the central impeller mid-plane and 1 cm apart from the wall. The tank is operated for 1 h ($Re = 20$) allowing the dye to disperse throughout the chaotic region of the tank, so that the asymptotic structure revealed by this injection appears as background. A second rhodamine injection is then released at the same location as before, while a third one is performed immediately afterward above the upper impeller, 5 cm from the shaft and 2.5 cm above the impeller mid-plane. The system is then examined using a laser sheet to expose mixing patterns in a 2-D vertical plane. Therefore, the areas illuminated by dye correspond to intersections of the laser sheet with the partially mixed structure. Figure 4 is a snapshot of this structure taken 10 min after the second injection. It is apparent that mixing does occur, although it is evidently inefficient. Only a small portion of the mixing area has been infiltrated after 10 min of agitation. The tracer streaks are attached to the unstable manifold of the flow, gradually invading the chaotic region of the tank, in an iterative process that progressively adds features to a stationary template (asymptotic directionality property). For this $Re$, the tank is divided into six weakly communicated flow cells. The transport between cells appears to occur through the manifold branches aligned to the walls and via descending or ascending ribbons observed around the impeller shaft. The sequence in which the compartments are connected is nontrivial. The central cells (third and fourth) share material through manifold branches aligned to the wall (Figure 3f). Material from the third cell ascends to the tank surface also via manifold branches aligned to the wall to later descend in a ribbon-like fashion to the uppermost impeller (see also Figure 3e) and be distributed within the first and second cells separated by ''broken separatrices.'' Similarly, material from the fourth compartment is transported to the sixth compartment and later to the fifth compartment. Within each cell, the flow is similar to the one observed for a single Rushton system. Each impeller conveys the fluid toward the walls radially. Recirculation loops are observed, as expected. The assumption of good mixing within each compartment is inaccurate, since within each cell we find a toroidal region of regular motion (dark regions at each compartment) completely isolated (in the convective sense) from the chaotic surroundings. Within these isolated regions, there exists also a complex structure as unveiled by the third injection (performed inside the uppermost regular torii) and the computational Poincaré section presented later in Figure 6a.

This LIF experiment also reveals clearly another characteristic structural feature of vessels agitated by impellers: trains of folds coming from impellers. The connection between these folds with mixing dynamics is discussed in detail in later sections. First, we examine the basic underlying motion that

originates the six-cell structure that we have described before.

### *Underlying regular structure*

If we replace the Rushton impellers by discs without blades, we expect to see a situation in which chaotic mixing is not possible for low *Re* since the flow field is effectively 2-D, that is, every azimuthal slice through the mixer is identical (see, for example, Strogatz, 1997; Fountain et al., 1998). However, the overall flow structure of a three-disc and a three-Rushton system may be expected to be similar, simply by realizing that from a geometric viewpoint, the blades can be regarded as a ''small'' perturbation of the three-disk geometry.

This expectation is confirmed by experiments performed under laminar flow conditions ($Re = 20$). A double injection of fluorescent dye is performed in the top portion of a three-disc system. First, green dye is injected and allowed to disperse for 10 min. Then, red dye is injected closer to the shaft. The sequence in Figures 5a–5c shows the time evolution of the mixing structure in the top portion of the tank. The green dye remains confined to the upper section of the tank, defining a toroidal structure. The red dye wraps around this torus, but no mixing occurs between the red and green dyes as they populate different layers of an ''onion-like'' family of nested torii. The complex filament structure evidenced in the figure, discussed in Shinbrot et al. (2001), is beyond the scope of this article.

Next, we explore the structure between the first and second discs. Figure 5d shows a 2-D laser cut through the experimental system injected with a fluorescent tracer (rhodamine) at two different locations, respectively, within the second and the third circulation cells. A stable structure exhibiting nested torii that do not mingle is revealed. These torii barely evolve with time; the image presented here (Figure 5d) shows the system 30 min after injection and exhibits no detectable change over tens of minutes. No communication is observed between the two cells. Figure 5e further resolves the onion-like internal pattern characteristic of the nested torii (only the top two compartments are illustrated). To reveal this structure, a tracer injection is performed in each flow compartment and the agitation is alternatively started and stopped, causing the dye to infiltrate concentric orbits during the transients and to stretch along the torii during steady agitation. This highly regular structure constitutes the underlying flow template present in a three-Rushton impeller stirred tank configuration.

Figures 6a and 6b show Poincaré sections of both a three-Rushton and a three-disc system constructed by computationally following the trajectories of 1,000 particles initially aligned between the shaft and the tank wall and recording their intersections with a fixed vertical plane. The overall structure revealed in this way is almost identical in both cases. Six compartments (Figure 6c) are defined within the tank in both cases (as revealed also by the previously discussed experiments). The separatrices between compartments are practically identical. Within each compartment, nested trajectories are revealed (see also Figure 5e). In this particular case Poincaré sections fail as a qualitative tool for the diagnosis of chaos in the three-Rushton system, since both sections appear very similar (an artifact caused by the weakly

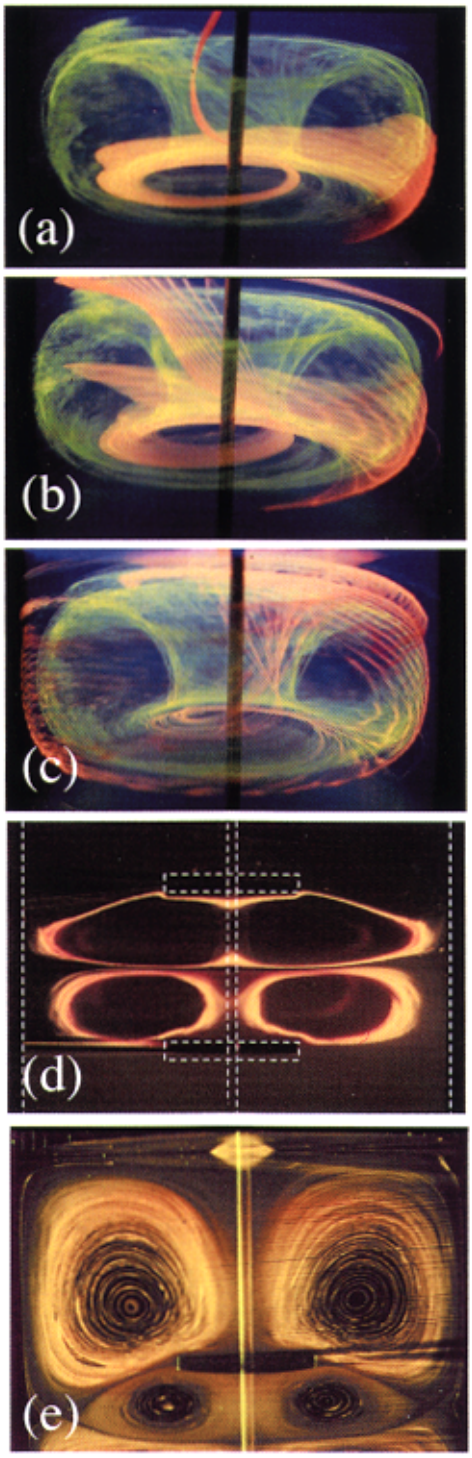


**Figure 5. Underlying regular structure in a three-impeller system.**

The evolution of structure in 3-D is revealed by a double injection UV visualization experiment in a three disc system at several different times: (a) 30 s, (b) 3 min, and (c) 5 min after the second injection (red dye); (d) LIF experiment in a three disc system showing the cross section of the structure resulting of two dye injections (at the second and third recirculation cells) of a three-disc system; (e) nested regular orbits in the first and second circulation cells in a three disc system.

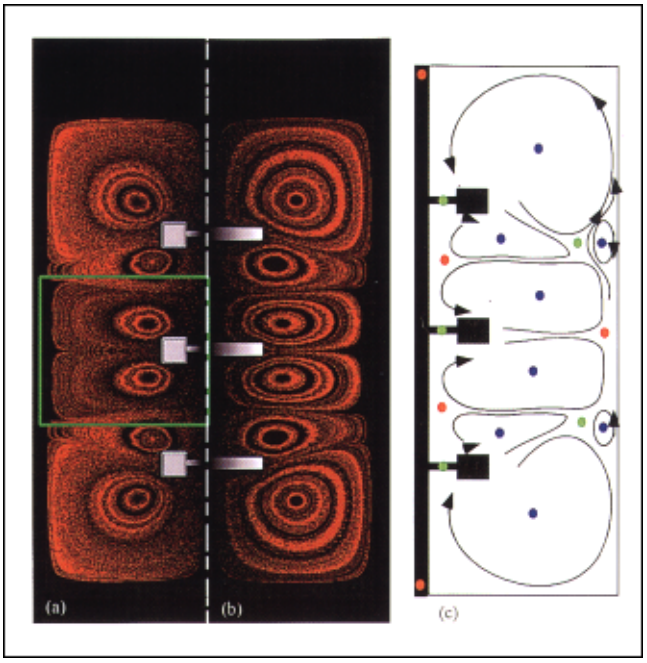


**Figure 6. Structural similarities between a three-Rushton and a three-disc tank system (*Re* = 20).**

(a) Surface of section for a three-Rushton system, and (b) for a three-disc system. (c) Flow structure and location of the elliptic (blue), parabolic (red), and hyperbolic (green) points.

chaotic nature of the flow and the difficulty of carrying long-term computations).

Another diagnostic tool, stretching plots, tells a better tale. Stretching is related to the micromixing intensities of a flow system. It measures the elongation potential of the flow on fluid elements computationally represented by infinitesimal

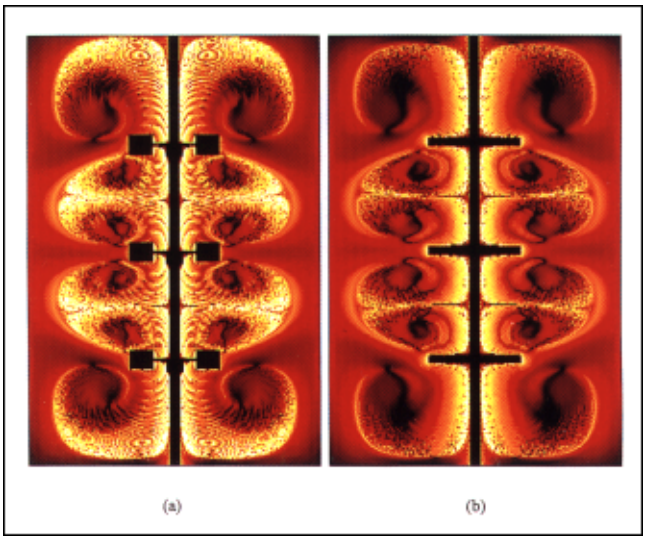


**Figure 7. Comparison of stretching fields for a three-Rushton impeller (a), and a three-disc impeller system (b) for *Re* = 20.**

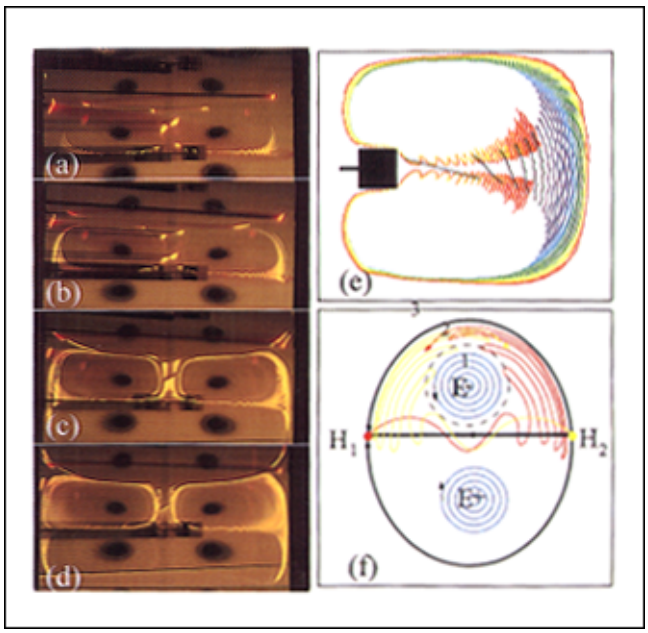


**Figure 8. Tracer dispersion patterns originated by the middle impeller in a three-Rushton system operated at *Re* = 20.**

From (a) to (d), a p-LIF experiment is presented. A first fluorescent pulse is injected in the chaotic region. After 3 h of agitation, the dye disperses within the chaotic region and only the islands of regular motion remain dark. A second dye injection is performed and its evolution in time is recorded: (a) 0.30 min; (b) 0.45 min; (c) 1.30 min; and (d) 3.00 min after the second injection. (e) The dye dispersion paths in the impeller vicinity are reproduced via simulation. (f) Perturbation of regular manifolds by the action of a sustained stimulus.

vectors (see, for example, Muzzio et al., 1992a,b). Since these vectors tend to align themselves to the unstable manifold of the flow, a plot of stretching values also renders information about the manifold structure (see, for example, Alvarez, 2000). Moreover, stretching fields are also time-invariant and can be used to predict other properties of interest, such as intermaterial area density and striation thickness distributions (Alvarez et al., 1998; Muzzio et al., 2000). Stretching fields are calculated (Figure 7) for both the three disc and the three Rushton cases at $Re = 20$ (for details, see Zalc et al., 2001). The same arbitrary scale of color, meant to enhance structural features, has been imposed in both cases. As in the case of the Poincaré sections, the structure reveals substantial similarity. For example, both of the systems are compartmentalized, the boundaries between these compartments are remarkably equivalent, and the centers of the circulation loops and the separatrices are coincident. However, some differences in local stretching topology can also be identified in Figure 7. Small striped patterns are observed at the shaft neighborhood for the three-impeller case, and the yellow stretching band appears to be thicker in the three-Rushton system.

In the following section, we examine in detail how the presence of blades causes these small-scale differences leading to partial chaos in the Rushton system.

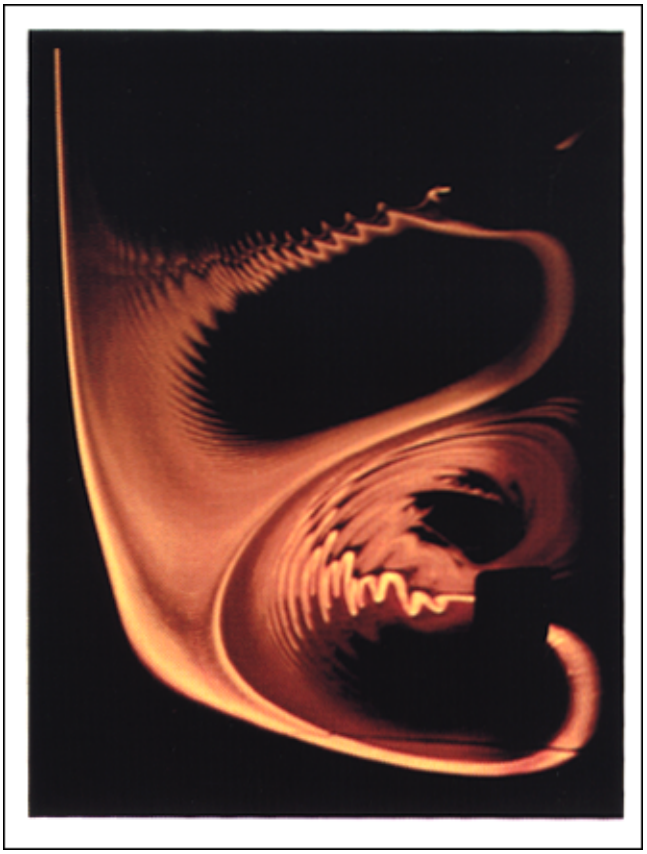

**Figure 9. P-LIF experiment showing the tracer dispersion trajectories generated by a three-Rushton system in which the third, fifth, and sixth blades of the middle impeller have been removed.**

Only the middle and top impellers are displayed. Dye enters below the middle impeller and is deformed by the passing blades. Since the blades remaining in the impeller are not equally spaced, the chain of folds exhibits different frequencies. The folds accumulate near the boundary of one of the compartments. The experiment was run at $Re = 30$.

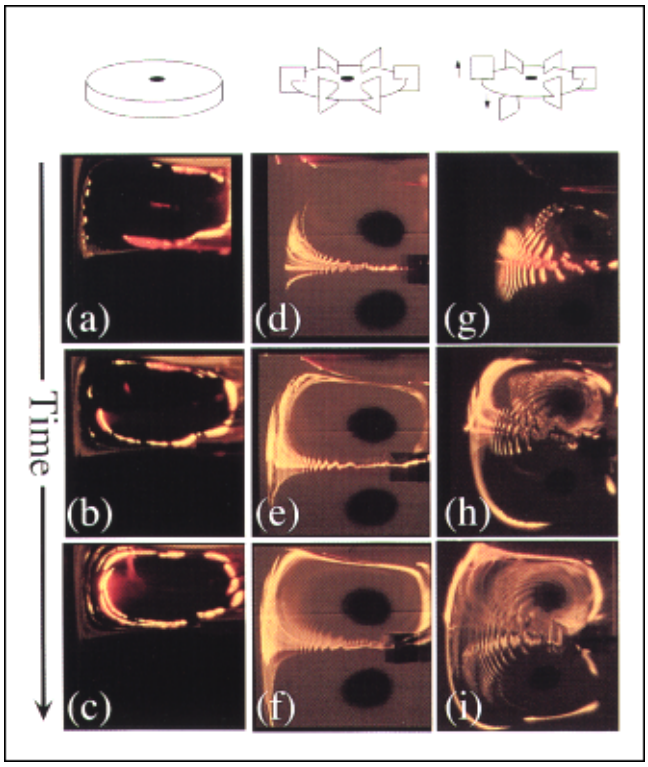


**Figure 10. Process of invasion of the chaotic region in the neighborhood of the middle impeller in a (a–c) three-disc system; (d–f) a normal three-Rushton system; and (g–i) a three-Rushton system in which the middle impeller has been modified by displacing one blade up and the next one down the disc plane.**

### *Role of the impeller blades: triggering chaos via perturbations*

We now focus on the events observed at the neighborhood of the impellers in a three-Rushton system. In Figure 8 we present snapshots corresponding to a pLIF experiment displaying the evolution in time of the intersection with a laser plane of a stream of dye initially injected close to the wall of the tank into the third circulation cell. In Figure 8a, we find a ribbon of dye descending around the shaft as it approaches the impeller (cf. Figure 3). When the ribbon reaches the impeller, it is propelled as a train of periodic folds toward the wall. A computer simulation recording the intersections of particle trajectories with a vertical plane in the tank reproduces the train of folds (Figure 8e). Each passage of a blade creates a fold that is convected radially along the impeller mid-plane. The frequency of the pulse is six times that of the impeller (consistent with the six-blade nature of the impellers used in the experiment).

The role of the blades in mixing can be understood in terms of the mechanism proposed by Beigie et al. (1994) for triggering chaos in 2-D flows. In fact, the flow structure observed in Figures 8a–8e is quite similar to the ''oscillating vortex pair,'' a 2-D model flow extensively studied a decade ago (see, for example, Beigie et al., 1991). Let us consider the flow structure represented by black lines in Figure 8f to be a simplistic representation of the base flow conditions in the neighborhood of the central impeller in the absence of blades. The elliptic points E+ and E− act as centers of the regular orbits depicted in blue ellipses. The unstable manifolds of the hyperbolic point H1 is exactly coincidental with the stable manifold of hyperbolic point H2. Such a steady 2-D flow exhibits no chaos and produces no mixing. However, a small sustained periodic perturbation applied in the neighborhood of H1 (as would be expected by the periodic passing of impeller blades) de-couples the manifolds, producing transverse heteroclinic intersections between the perturbed unstable (red) manifold and the perturbed stable (yellow) manifold of H2. These transverse intersections are a hallmark of chaos (Doherty and Ottino, 1988; Wiggins, 1992). In Figure 8f, some of the orbits around E− are not disturbed (represented in blue), while more distant ones are increasingly affected by the perturbation. We stress that the emergence of chaos—and the corresponding onset of mixing—in the Rushton system

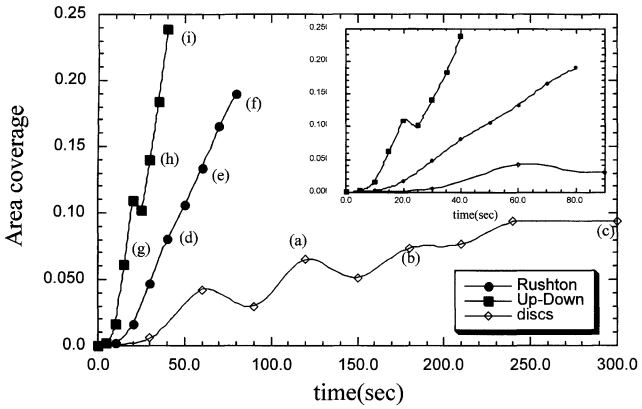


**Figure 11. Rate of dye invasion of the chaotic region on the neighborhood of the middle impeller for the systems referred to in Figure 10 calculated by image analysis of series of snapshots of the process of invasion.**

The letters from (a) to (i) are consistent with the sequence of frames shown in Figure 10.

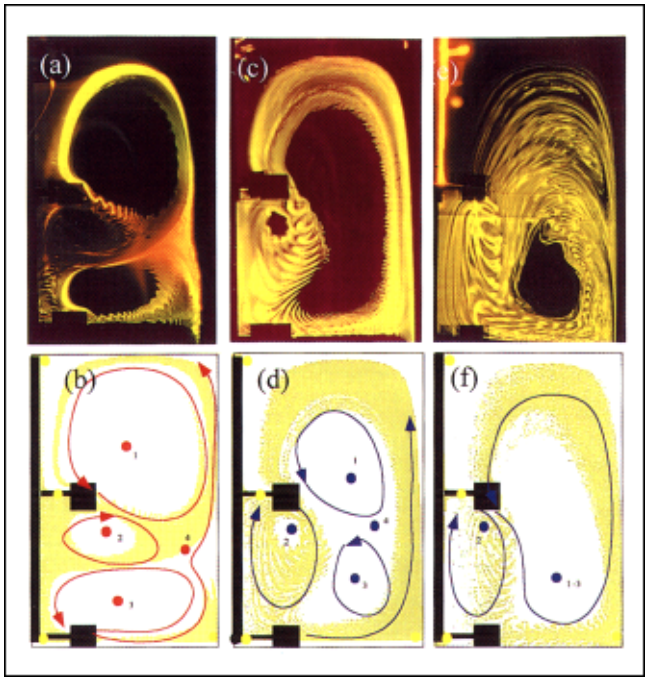


**Figure 12. Flow structure at different *Re* in stirred tank agitated by three-Rushton impellers, as revealed by p-LIF experiments (top sequence) and tracer injection computations (bottom sequence).**

Snapshots corresponding to $Re = 20$ (a–b), $Re = 40$ (c–d), and $Re = 80$ (e–f) are presented. On the computational sequence, elliptic (1,2,3) and hyperbolic points (rings) of the flow (4) have been marked. Arrows indicate flow circulation. Only the right top portion of a cross section is presented (region between the surface of the tank and the central impeller).

arises from small perturbations to an underlying flow largely similar to the one produced by discs.

Indeed, the effect on the regular underlying structure depends on the magnitude of the perturbation. Figure 9 shows the result of a p-LIF visualization experiment ($Re = 25$) in which the middle Rushton impeller has been mutilated (only the middle and top impellers are shown in the figure); the third, fifth and sixth blades have been removed (see Figure 1e). If an interval of motion (T) is defined as the time between the passage of regularly spaced blades, then the top impeller still generates 1T folds, while the waves generated by the middle impeller reflect three different characteristic periods: 1T, 2T, and 3T (see the M shape of the train of folds).

This result further confirms that the blades are directly responsible for the generation of the train of folds observed in Figure 8. However, it remains to be proven that these folds play a role in the occurrence of chaos and the development of mixing.

Let us analyze the evolution of the structure in the neighborhood of the central stirrer for three different stirrer geometries. Figure 10 shows time-series of p-LIF snapshots for a disc (a–c), a standard Rushton impeller (d–f), and an altered Rushton impeller in which the first blade has been moved up and the second down with respect to the midplane (g–i). By digitizing these photographs, we can quantitatively compare mixing rates. Images corresponding to different mixing times were thresholded and the fraction of pixels with intensity values above the threshold (representing the intersections of the dye stream with the laser plane) was calculated for each snapshot. The results of this procedure are presented in Figure 11.

As established before, for steady flow conditions, concentrically placed discs are incapable of producing chaotic mixing. The injected dye circulates in closed isolated flow envelopes. Eventually, by virtue of linear convective transport within envelopes, the injected dye completely infiltrates a given set of torii and their entire cross section appears bright. At that point, no further increase in area coverage is observed, since no convective transport between torii is possible. In the case of the Rushton impeller the area visited by the dye grows much faster than for disks. However, most of the dye remains in the compartment above the second impeller mid-plane. Eventually, the filament fills the chaotic portion of the third compartment, and slowly invades other compartments (c.f. Figure 4).

Finally, Figures 10g–10i show the time evolution of the dye stream in the vicinity of a modified Rushton turbine (one of the blades has been displaced above and an adjacent blade below the impeller mid-plane). The area invaded by the dye grows even faster and to a much higher asymptotic coverage value than when a standard Rushton configuration is used (see quantitative comparison in Figure 11). Thus, the chaotic region of the third compartment is quickly and almost completely filled, and the separatrix caused by that slight modification in impeller design can significantly enhance the perturbing action of the blades.

The results discussed so far imply that concentric stirred tanks in the laminar regime mix only by virtue of small perturbations generated by the periodic passing of the blades, a mechanism that triggers chaos in an otherwise completely regular and integrable flow system observed when concentric discs are used as impellers. From the geometrical point of

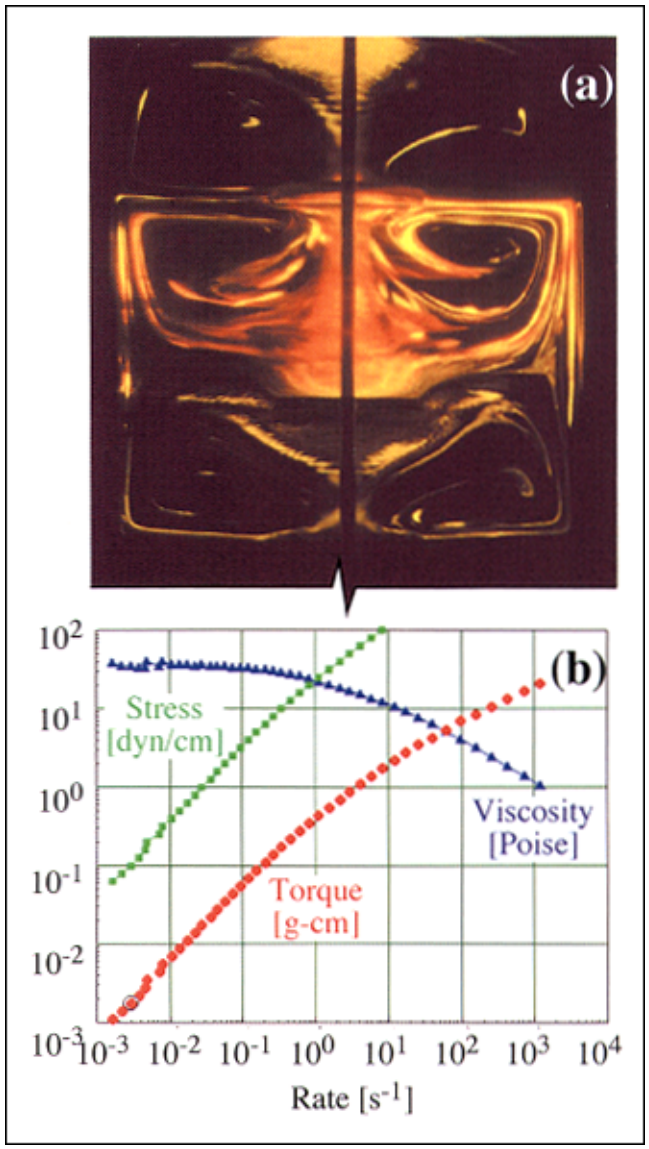


**Figure 13. Mixing of a non-Newtonian shear thinning (and slightly viscoelastic) fluid in a three-disc system (1% CMC solution in water; 100 rpm).**

(a) Nonlinear rheology of the fluid triggers chaos in a concentric three-disc tank system. In (b), the variation of the effective viscosity ($\eta$) of the fluid as a function of shear rate is shown.

view, the blades introduce only a minor perturbation; the total surface area that drives the mixing process (the blades area) is rather small (18 $cm^2$). From the energetic point of view, the same observation holds true. Based on the 3-D velocity field obtained via simulations, it is possible to calculate the total kinetic energy involved in driving both the three disc and the three Rushton cases at $Re = 20$ (for details on this calculation see Zalc, 2000). Comparatively, the mechanical energy invested in the operation of the Rushton system is only 1% higher than the one needed to drive the disc system. In other words, since the flows are nearly identical, most of the energy injected to a stirred tank system is used in irrelevant (from the mixing point of view) circulatory motion, and only 1% of it really contributes to mixing.

### *Other geometrical issues: the role of the compartment boundaries*

Let us now discuss the role of the compartment boundaries by examining again the experimental sequence presented in Figures 8a–8d. Once close to the wall, the amplitude of the folds is magnified and the chain of folds is packed, reoriented around a loop and re-injected toward the impeller (see also Figure 8e). As a consequence, during a subsequent cycle, each one of the original folds generates two new chains, following a classic horseshoe map (Figure 8d). The process is, therefore multiplicative, and the resulting mixing rate is exponential. The same phenomenon is also observed in Figure 9, except that now, for folds generated by the lower impeller, the boundary of the motion cell is not the tank wall, but the separatrix resulting from the interaction between the top and the middle impeller.

All of the elements of chaotic mixing are present here: flow perturbations, time periodicity, stretching, reorientation and iteration. Each one of these components is associated with geometrical features of the system. Reorientation and periodic time dependence are clearly caused by the passage of the blades. It is also the action of the blades that produces

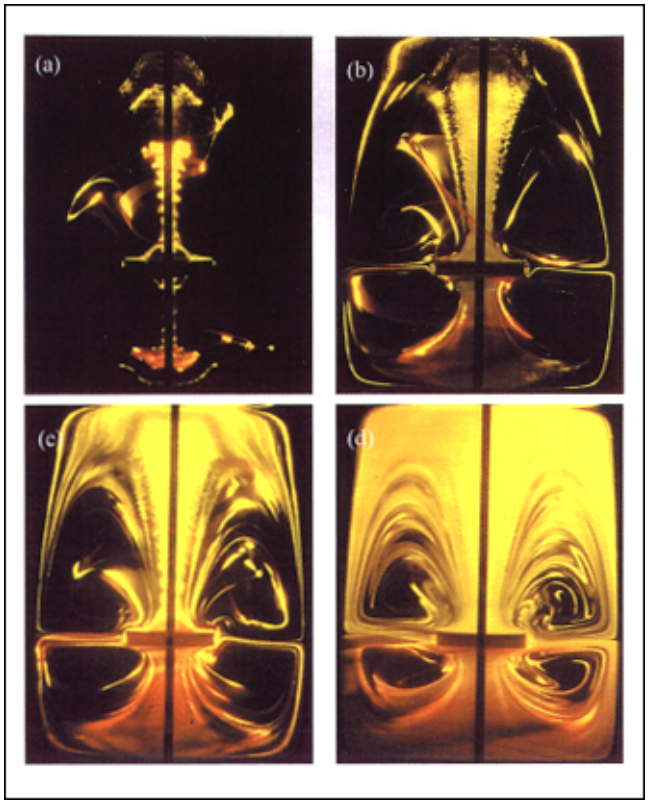


**Figure 14. Evolution of the partially mixed structure of a non-Newtonian liquid (1% CMC in water) agitated by a single concentric disc at 100 rpm.**

(a) 2 min; (b) 5 min; (c) 15 min; and (d) 45 min after injection of fluorescent dye.

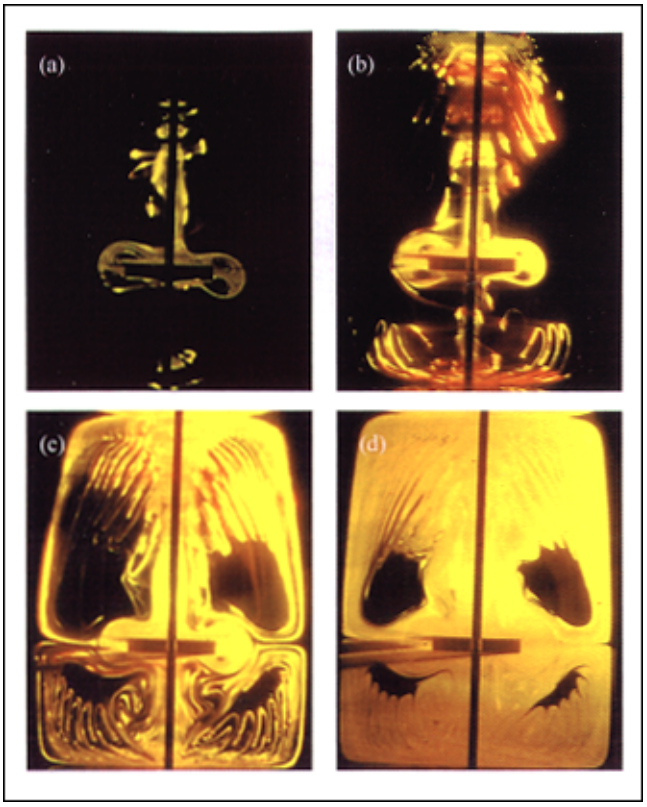


**Figure 15. Evolution of the partially mixed structure of a non-Newtonian liquid (1% CMC in water) agitated by a single concentric disc at 300 rpm.**

(a) 1 min; (b) 5 min; (c) 10 min; and (d) 30 min after injection of fluorescent dye.

folding and stretching in the tangential direction. Stretching in the vertical direction is caused by the accumulation of folds near critical points (rings). This fact is better appreciated when the dispersion process in 3-D is analyzed (Figures 3a and 3c). A ribbon approaches the impeller from above or below the impeller, and the passing of the blades elongates it into a thin sheet that is projected in a spiral to the wall. The interaction of the train of pulses with any form of compartment boundary of the system causes packing of material lines and additional stretching (this time in the cross-sectional direction). The circulatory motion in the tank forces the elongated sheet to be reoriented and repeatedly reinjected to the source of perturbation. As a consequence, an iterative horseshoe map with exponential stretching properties is originated. The presence of this horseshoe is depicted in the sequence of folds numbered 1,2,3, in Figure 8f.

Although the events previously described possess a general character for laminar concentric impeller systems, the overall geometric features of the flow are determined by the spacing between impellers (Harvey et al., 1996) and the intensity of the velocity field (such as the shape of the compartments in the region shown by Figure 8 is different to those found in Figure 9). Here, we discuss briefly the second issue.

Figure 12 shows details of partially mixed structures observed in the three-Rushton system under three different conditions: $Re = 20$ (Figures 12a–12b), $Re = 40$ (Figures 12c–12d), and $Re = 80$ (Figures 12e–12f). Experimental and computational results are presented side by side. Throughout this $Re$ range, the system undergoes remarkable global structural changes. For example, the center of the second isolated region from top to bottom observed at $Re = 20$ shifts inward as $Re$ increases (see displacement of elliptic point 2 in Figures 12b, 12d, and 12f. At $Re = 40$, the uppermost elliptic ring begins a migration downward. In fact, at early stages of the mixing process, the first and third cells look like a single large isolated region. However, at later mixing stages, two independent isolated regions can be differentiated and a Poincaré analysis (not shown here) reveals the presence of two distinct elliptic points (Zalc et al., 2001). At $Re = 80$, the elliptic points 1 and 3 merge completely (elliptic points 1–3 in Figure 12f). As a result, the first and third isolated regions in Figure 12a now share a common KAM surface surrounding them and the whole flow changes from a six cell structure to a four cell structure.

Also, the amplitude of the wiggles originating from the top impeller is greatly increased as $Re$ increases (the magnitude of the perturbation increases), and, as a consequence, the size of the segregated areas decreases (see also Zalc et al., 2001). The overall changes in flow circulation during this bifurcation are sketched in Figures 12b, 12d, and 12f. During the course of this event, as $Re$ is increased from 20 to 80, one hyperbolic point (ring) has vanished (point 4) and one elliptic point (ring) has disappeared (resulting from the merging of 1 and 3), conserving the topological index of the system. (The topological index (TI) of a dynamical system is calculated by adding 1 for each hyperbolic point in the system, subtracting 1 for each ellipic periodic point, and adding 1/2 for each parabolic point ($TI = \Sigma H - \Sigma E + 1/2\Sigma P$). Through bifurcations, the topological index of the system must be conserved.)

### *Chaos in non-Newtonian systems*

Up to this point, we have excluded from our discussion the role of complex rheological behavior in the creation of microstructure by focusing only on Newtonian fluids. However, rheology does play an important role, especially in laminar mixing processes. The flow properties (such as apparent viscosity) of a non-Newtonian liquid depend on the shear rate. Since the distribution of shear rates within a stirred tank spans several orders of magnitude (see, for example, Lamberto et al., 1999), a wide spectrum of local viscosity conditions is expected, adding complexity to the physical picture. Moreover, the dependence of the viscosity on the velocity field and the history effects (for viscoelastic fluids) adds nonlinearity to the equations of motion. This added nonlinearity can amplify small asymmetries of the system (slight misalignment of impellers or shafts) that otherwise would be inconsequential. To illustrate this, we present here experiments performed using a 1% carboxy-methyl cellulose solution, a shear-thinning liquid with weak viscoelastic properties (see Figure 13).

Figure 13 presents an experiment in which a system with three concentric discs rotating at 200 rpm is used to stir this fluid. The snapshot corresponds to 10 min after an injection is performed at the third tank cell. Experiments performed using Newtonian fluids under otherwise identical conditions display a complete absence of chaos. For the non-Newtonian case, however, the dye injection (Rhodamine in this case) does

not remain confined to regular orbits, but invades progressively the different compartments of the system and wiggling motion is observed in particular locations of the system.

Figures 14 and 15 show LIF snapshots of dye dispersion experiments in a single disc system at 100 rpm and 300 rpm, respectively. At 100 rpm, the flow direction characteristic of Newtonian radial systems (from the impeller to the walls) is inverted (Nienow and Elson, 1988). The dye flows from the walls to the impeller and ''climbs'' up and down the shaft (see Figure 14c) and wiggling motion can be observed in the shaft vicinity. We hypothesize that these wiggles are originated by the minor misalignment of the disc to the horizontal plane, and magnified by the nonlinearity of the rheological behavior of the fluid. After injection near the disk, the flow convects the dye to the top of the tank and recirculates it along the tank walls to the mid-plane separatrix and toward the impeller, where the filament of dyed fluid is re-injected to the loop to create a finer and finer lamellar pattern that asymptotically covers the whole chaotic domain. At 300 rpm, the flow field is considerably more complicated. In the immediate disc neighborhood, flow away from the impeller is observed (see Figure 15c). Within this region of ''normal radial flow,'' areas of slow mixing are detectable slightly above and below the disc. However, in the rest of the system the direction of the flow is reverted. Pockets of fluid travel away from the disk up and down the impeller shaft, and are recirculated along the walls. Folding lobes are generated (see Figure 15) due to the interaction of the fluid with the bottom or the top of the tank.

These lobes intrude the body of the flow domain, but do not cover the cross section of the tank entirely, leaving unreached segregated regions above and below the disc even after 15 min of mixing. Interesting dynamical behavior is also revealed in Figure 16. Different from a Newtonian system, the mixing structure is not ''steady.'' When illuminated with a laser sheet, a Newtonian system displays a structure which evolves in time adding detail to an invariant basic skeleton (see, for example, Figure 7). However, in the non-Newtonian system we describe here, the same experiment will reveal a mixing structure that oscillates periodically. Figures 16a–16d are consecutive snapshots of the partially mixed structure evolving in a vessel containing 1% CMC agitated by a single concentric disc at 400 rpm. Between frames, there is a lapse of 0.051 s. Three parallel lines have been drawn as a refer-

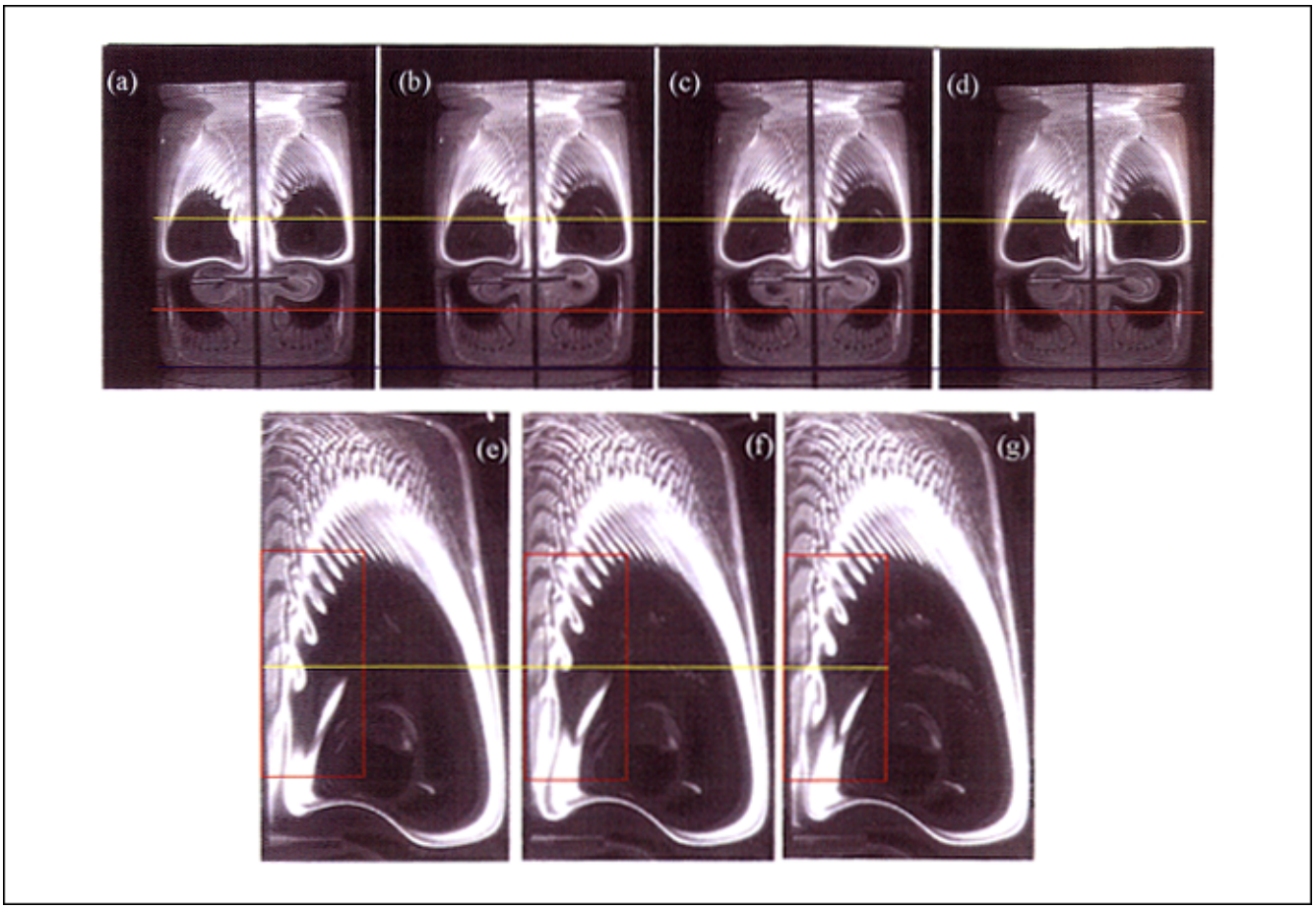


**Figure 16. The sequence from (a)–(d) corresponds to a series of consecutive snap shots taken with a high-speed CCD camera (0.051 s apart from each other) to a non-Newtonian mixing system (CMC 1% stirred at 400 rpm with a concentric disc).**

From (e)–(g), a sequence corresponding to an agitation rate of 300 rpm is presented. The lines and frames are intended as references to facilitate the comparison of the structural features.

ence. The reader can observe that the structure moves in time, but returns to the same configuration after three frames (Figures 16a and 16d) are practically identical. The bottom sequence in Figure 16 shows a closeup of a region in the neighborhood of the disc in a non-Newtonian system agitated at 300 rpm. A train of folds is originated at the juncture between impeller and shaft. The sequence captures the advance of the train of folds, revealing again periodic rather than invariant dynamics. Still, even when the observed structure is not invariant for a specific plane of the tank, the asymptotic directionality property holds, since periodically the same template will reappear (with more detail added) in a particular plane.

## Concluding Remarks

In this article we communicate a surprisingly wide repertoire of mixing phenomena that have previously been described and studied only for model 2-D flows. We explored the mechanisms for the onset of chaos in laminar stirred tanks, all of them related to a fundamental concept: the effect of sustained perturbations over a regular base flow.

First, we show that in typical concentric configurations, chaos is generated as a result of the periodic perturbation that the impeller blades exert on an underlying regular structure generated by an otherwise integrable flow that is observed when discs are used to drive the flow. This is a case in which design led by intuition rendered success. Certainly, the use of a disc with blades to mix was not inspired in chaos theory, and, yet, the idea has proven to be useful. Still, the fact that the ''perturbed'' design is so close to integrability explains the poor mixing performance displayed by typical stirred tank configuration in laminar regimes. Most of the energy invested in the operation of a stirred tank is consumed in generating the rotational motion of the fluid, which is completely unfruitful in terms of mixing.

Can we do better by knowing that it is the bending of filaments caused by the passing of the blades what really causes mixing in a stirred tank? Conceptually, we should. Once the mechanism is known, it can be used in several ways: wider blades may introduce larger disturbances, asymmetric arrays of the blades around the impeller disc can generate multifrequency waves, and so on.

We also briefly analyzed the case of mixing in non-Newtonian systems, finding that the nonlinearities on the rheological behavior of the liquid (in this case a shear-thinning and viscoelastic fluid) can amplify small disturbances in the system, once again triggering chaos.

An essential qualitative observation from the experiments presented here is that chaos triggered by flow perturbations in stirred tanks generates self-similar mixing patterns controlled by asymptotic directionality (AD) independently of the fluid being Newtonian or Non-Newtonian. This observation is important because, heretofore, AD has only been proved to be required for reversible flows. Since flows in stirred tanks are irreversible, our experimental results suggest that reversibility is not a necessary condition for AD, suggesting the existence of a universal template for chaotic mixing processes, whether driven or spontaneous. This observation, which has important consequences, will be examined rigorously in future publications.

In a summary, stirred tanks are a 3-D example of the well-known fact in the area of nonlinear dynamics that a small sustain perturbation can trigger chaos in an integrable 2-D system.

## Literature Cited


Alvarez, M. M., ''Using Spatio-Temporal Asymmetry to Enhance Mixing in Chaotic Flows: from Maps to Stirred Tanks,'' PhD Diss., Rutgers University (2000).

Alvarez, M. M., F. J. Muzzio, S. Cerbelli, A. Adrover, and M. Giona, ''Self-Similar Spatiotemporal Structure of Intermaterial Boundaries in Chaotic Flows,'' *Phys. Rev. Lett.*, **81**, 3395 (1998).

Aref, H., ''Stirring by Chaotic Advection,'' *J. Fluid Mech.*, **143**, 1 (1984).

Beigie, D., A. Leonard, and S. Wiggins, ''Chaotic Transport in the Homoclinic and Heteroclinic Tangle Regions of Quasiperiodically Forced Two-Dimensional Dynamical Systems,'' *Nonlinearity*, **4**, 775 (1991).

Beigie, D., A. Leonard, and S. Wiggins, ''Invariant Manifold Templates for Chaotic Advection,'' *Chaos, Solitons and Fractals*, **4**, 749 (1994).

Doherty, M. F., and J. M. Ottino, ''Chaos in Deterministic Systems: Strange Attractors, Turbulence, and Applications in Chemical Engineering,'' *Chem. Eng. Sci.*, **43**, 139 (1988).

Fountain, G. O., D. V. Khakhar, and J. M. Ottino, ''Visualization of Three-Dimensional Chaos,'' *Science*, **281**, 683 (1998).

Harnby, N., M. F. Edwards, and A. W. Nienow, *Mixing in the Process Industries*, Butterworth-Heinemann, NY (1992).

Harvey III, A. D., C. K. Lee, and S. E. Rogers, ''Steady-State Modeling and Experimental Measurement of a Baffled Impeller Stirred Tank,'' *AIChE J.*, **41**, 2177 (1995).

Harvey III, A. D., S. P. Wood, and D. E. Leng, ''Experimental and Computational Study of Multiple Impeller Flows,'' *Chem. Eng. Sci.*, **52**, 1479 (1997).

Harvey III, A. D., D. H. West, and N. B. Tufillaro, ''Evaluation of Laminar Mixing in Stirred Tanks Using a Discrete-Time Particle-Mapping Procedure,'' *Chem. Eng. Sci.*, **55**, 667 (2000).

Hobbs, D. M., M. M. Alvarez, and F. J. Muzzio, ''Mixing in Globally Chaotic Flows: A Self-Similar Process,'' *Fractals*, **5**, 1 (1997).

Lamberto, D. J., F. J. Muzzio, P. D. Swanson, and A. L. Tonkovic, ''Using Time-Dependent RPM to Enhance Mixing in Stirred Vessels,'' *Chem. Eng. Sci.*, **51**, 733 (1996).

Lamberto, D. J., ''Enhancing Laminar Mixing in Stirred Tank Reactors Using Dynamic Flow Perturbations,'' PhD Thesis Diss., Rutgers University (1997).

Lamberto, D. J., M. M. Alvarez, and F. J. Muzzio, ''Experimental and Computational Investigation of the Laminar Flow Structure in a Stirred Tank,'' *Chem. Eng. Sci.*, **54**, 919 (1999).

Lamberto, D. J., M. M. Alvarez, and F. J. Muzzio, ''Computational Analysis of Regular and Chaotic Mixing in a Stirred Tank Reactor,'' *Chem. Eng. Sci.*, in press (2000).

MacKay, R. S., J. D. Meiss, and I. C. Percival, ''Transport in Hamiltonian Systems,'' *Physica D*, **33**, 55 (1993).

MacKay, R. S., ''Transport in 3D Volume-Preserving Flows,'' *J. Nonlin. Sci.*, **4**, 329 (1994).

Metzner, A. B., and J. S. Taylor, ''Flow Patterns in Agitated Vessels,'' *AIChE. J.*, **6**, 109 (1960).

Muzzio, F. J., M. M. Alvarez, S. Cerbelli, M. Giona, and A. Adrover, ''The Intermaterial Area Density and Striation Thickness Distribution Generated by Time- and Spatially-Periodic 2D Chaotic Flows,'' *Chem. Eng. Sci.*, **55**, 1497 (2000).

Muzzio, F. J., C. Meneveau, P. D. Swanson, and J. M. Ottino, ''Scaling and Multifractal Properties of Mixing in Chaotic Flows,'' *Phys. Fluids A.*, **4**, 1439 (1992a).

Muzzio, F. J., P. D. Swanson, and J. M. Ottino, ''Mixing Distributions Produced by Multiplicative Stretching in Chaotic Flows,'' *Int. J. Bif.* & *Chaos*, **2**, 37 (1992b).

Nienow, A. W., and T. P. Elson, ''Aspects of Mixing in Rheologically Complex Fluids,'' *Chem. Eng. Res.* & *Design*, **66**, 5 (1988).

Ottino, J. M., *The Kinematics of Mixing: Stretching, Chaos, and Transport*, Cambridge University Press, Cambridge (1989).

Shinbrot, T., M. M. Alvarez, J. M. Zalc, and F. J. Muzzio, ''Attraction of Minute Particles to Invariant Regions of Volume Preserving Flows by Transients,'' *Phys. Rev. Lett.*, **86**, 1207 (2001).
Strogatz, S. H., *Nonlinear Dynamics and Chaos; with applications to Physics, Biology, Chemistry, and Engineering*, Perseus Books, Reading, MA (1994).
Wiggins, S., *Chaotic Transport in Dynamical Systems*, Springer-Verlag, New York (1992).
Zalc, J., ''Computational Fluid Dynamics (CFD) Tools for Investigating Flow and Mixing in Industrial Systems: The Koch-Glitsch SMX Static Mixer and a Three Rushton Turbine Stirred Tank,'' PhD Diss., Rutgers University (2000).
Zalc, J. M., M. M. Alvarez, T. Shinbrot, B. E. Arik, and F. J. Muzzio, ''Extensive Validation of Computed Laminar Flow Fields in a Stirred Tank Equipped with Three Rushton Turbines,'' *AIChE J.*, **47**, 2144 (2001).

*Manuscript received Sept. 5, 2001, and revision received Feb. 12, 2002.*